Effect of MYC and PARP Inhibitors in Ovarian Cancer Using an *In Vitro* Model

ALESSANDRO MOREA[1], SAYEH SARAVI[2], CRISTINA SISU[2], MARCIA HALL[3], SABRINA TOSI[2], EMMANOUIL KARTERIS[2#] and CLELIA TIZIANA STORLAZZI[4#]

[1]IFOM Institute, Milan, Italy;

[2]Department of Life Sciences, College of Health, Medicine and Life Sciences, Brunel University London, Uxbridge, U.K.;

[3]Mount Vernon Cancer Centre, Northwood, U.K.;

[4]Department of Biosciences, Biotechnology and Environment, University of Bari Aldo Moro, Bari, Italy

[#]These Authors contributed equally to this study.

***Correspondence to*:** Emmanouil Karteris, Division of Biosciences, Department of Life Sciences, College of Health, Medicine and Life Sciences, Brunel University London, Uxbridge, UB83PH, U.K. Tel: +44 1895265892, e-mail: Emmanouil.Karteris@brunel.ac.uk; Clelia Tiziana Storlazzi, Department of Biosciences, Biotechnology and Environment, University of Bari Aldo Moro, Via Giacomo Tauro, n.3/D, 70124, Bari, Italy. Tel: +39 0805443582, e-mail: cleliatiziana.storlazzi@uniba.it

Key Words: Ovarian cancer, *MYC*, *PVT1*, circPVT1, MYC inhibitor, rucaparib.

Running title: Effect of MYC and PARP Inhibitors in Ovarian Cancer

Experimental Study

Abstract

Background/Aim: The 8q24 chromosomal region, which contains the *MYC* and *PVT1* candidate oncogenes, is amplified in carcinomas. Both genes have been involved in the etiopathogenesis of ovarian cancer (OC). In this study, we used an *in vitro* OC model with a known 8q24 copy number increase and *in silico* tools to investigate the expression of *MYC/PVT1* loci and copy number variation in OC. We also assessed the effects of Rucaparib (a PARP inhibitor) in the presence or absence of 10058F4 (a MYC inhibitor) on the expression of *MYC*/linear *PVT1*/circular PVT1. **Materials and Methods:** Tissue culture, chromosome preparation, RNA extraction, RT-qPCR, FISH, and wound healing assays were employed. OncoDB, cBioportal, UALKAN, and ROC Plotter *in silico* tools were also utilized. **Results:** Although *PVT1* and *MYC* expression levels remained unaltered in OC, putative copy number alterations across all cancers showed a marked difference between the two genes, particularly in gain and amplification for *MYC*. *PVT1* expression demonstrated prognostic value for the treatment of patients with serous and endometrioid OC. Both genes correlated with *PARP10*, *FAM83H,* and *DEPTOR.* The use of Rucaparib in the presence or absence of the MYC inhibitor (10058F4) *in vitro*, led to a significant down-regulation in the expression of *MYC*, linear, and circular *PVT1*. **Conclusion:** Our data provide a novel insight into the potential interactions of *MYC* and *PVT1* with other genes. Moreover, we identified a new PARP inhibition mechanism down-regulating *MYC*, as well as the linear and the circular *PVT1* transcripts. Future work should expand on clinical studies to better understand the prognostic role of *PVT1* in OC.

Deletions and amplifications are commonly found in advanced tumor stages. In particular, the 8q24 chromosomal region is frequently amplified in carcinomas. Emerging studies demonstrate that this amplification in ovarian and breast cancers is associated with reduced patient survival (1). This effect is primarily due to the role of the *MYC* oncogene, mapping at 8q24.21, encoding for a nuclear transcription factor; it has been implicated in the malignant progression of various human tumors (2), including ovarian cancer (OC). Indeed, numerous studies have investigated *MYC* copy number variation (CNV) in OC and their correlation with clinicopathological parameters using fluorescence *in situ* hybridization (FISH). For example, in 30% of gynecological malignancies, like endometrioid and epithelial OC, *MYC* amplification is evident, and there is an association between OC malignancy and *MYC* CNV (3).

Another emerging candidate oncogene mapping at the same chromosomal region is the long non-coding RNA gene plasmacytoma variability translocation 1 (*PVT1*). Consistent with its association with various types of cancer, its expression is regulated by TP53 through a canonical p53-binding site (4) and has been implicated in regulating MYC levels (5) to promote tumorigenesis (6, 7). *PVT1* maps to 52 Kb downstream of the *MYC* locus, and it is about 300 Kb pairs in size (8). Interestingly, patients and cell lines with a high copy number gain of *MYC* and *PVT1* show a higher expression of the hsa_circ_0001821 circular RNA (*circRNA*) obtained from the back splicing of *PVT1* exon 2 (circPVT1) than in samples without 8q24 high-copy number gain (9, 10). circPVT1 is presently described as involved in inducing cell proliferation and tumorigenesis. Notably, it is reported as crucial in multiple tumor types, including OC, and there is evidence that it enhances cell proliferation and drug resistance, and inhibits apoptosis. Indeed, it might have a role as a miRNA sponge, as documented for several miRNAs, considering it is enriched in the cytoplasm of tumor cells. Notably,

circPVT1 could play an essential role in OC as a sponge of miR-149-5p, leading to the Forkhead Box M1 (FOXM1) over-expression. Furthermore, recent evidence excluded its translation into a functional protein since its longest ORF did not produce a detectable protein at the western blotting level (11).

The role of *PVT1*/circPVT1 and the interplay with *MYC* is still under investigation (12). As mentioned, *MYC* and *PVT1* contribute independently to ovarian pathogenesis when over-expressed due to genomic abnormalities (1). Moreover, silencing *PVT1 in vitro* impaired cell proliferation, migration, and invasion (13). These data are of particular significance, given that OC affects over 300,000 women globally, accounting for more deaths than any other cancer of the female reproductive system (14). Here, we used an *in vitro* OC model with a known 8q24 low-copy number amplification and *in silico* tools to investigate the expression of *MYC/PVT1* loci and CNV in OC. Furthermore, we assessed the effects of Rucaparib (a PARP inhibitor) in the presence or absence of 10058F4 (a MYC inhibitor) on the expression of *MYC/PVT1*/circPVT1 using RT-qPCR.

Materials and Methods

Tissue culture. In this study, we used the SKOV3 cell line (ECAAC 91091004), considered a serous OC cell line characterized by adherent and hypo-diploid cells derived from a patient with OC. The cell line was cultured in T75 cell flasks with a filter head (Nunc; Life Technologies Ltd, Paisley, UK), supplemented with 10% fetal bovine serum and 1% penicillin-streptomycin (Fisher Scientific, Leicestershire, UK). Cells were incubated at 37ºC in a humidified atmosphere of 5% CO2 in the air. Cells were

subcultured every two or three days at 80-90% confluency by trypsinization with Tryple Express (TrypLE Express, Gibco).

Chromosome preparations. Chromosome suspensions were obtained from SKOV-3 cultured cells using standard protocols (15). Briefly, colcemid (0.05 μg/ml) was added to cell cultures 1 h before harvesting. Then, cells were treated with hypotonic solution (KCl, 0.075 M) and fixed with methanol-acetic acid (3:1). Fixed chromosome suspensions were stored at -20°C until spread on microscope slides.

RNA extraction/RT-qPCR. Cells were plated in a 6-well plate and then treated in a dose- and time-dependent manner with DMSO (0.1%), PARP inhibitor (Rucaparib), and MYC inhibitor (10058F4). RNA was extracted using the RNeasy Mini Kit (Qiagen, Manchester, UK). cDNA was synthesized from mRNA utilizing cDNA reverse transcription (Life Technologies). cDNA concentration was measured using RNA concentrations defined by Nano-Drop 2000C (Life Technologies). Relative expression of the genes of interest was measured using quantitative PCR (qPCR) on QPCR QuantStudio 7 Flex Real-Time PCR machine using SYBR® Green PCR Master Mix (Life Technologies) using primers detailed in Table I for *PVT1* and *MYC*, using *YWHAZ* as a housekeeping gene. The three primer pairs used for the MYC gene could detect all possible splicing variants so far mapped for MYC (UCSC GRCh38/hg38 release). Relative quantities (RQ) values were calculated using the comparative $2^{-\Delta\Delta Ct}$ analysis method (16).

Wound-healing assay. Wound healing assay was performed to assess the cell ability to close a created gap in the cell growth area. A ‘scratch’ was made, as a line drawn on one part of the well, by using a 200 μl pipette tip. In the following step, closure of the scratch was monitored, and images were taken after 24, 48 and 72 h using a Leica

DMi1 inverted microscope (40× magnifications; Leica Microsystems, Milton Keynes, UK). The perpendicular line of the marker was used as a landmark to ensure that an image of the same area was taken at each time point. All images were analyzed with ImageJ.

In silico analyses. Xena Functional Genomics Explorer from the University of California Santa Cruz (UCSC) was accessed, and in particular, The Cancer Genome Atlas (TCGA) dataset, to study correlations between the OC cohort samples and healthy ovarian tissue cohort (GTEX-samples). These datasets are enriched with information from studies from different research groups all over the world, thanks to the project called Genomic Data Common Data Portal (GDC) by the National Cancer Institute (NIH), to collect information for each cancer type. The analysis focused on assessing differential gene expression and copy number variations between cancer and the healthy situation, underlining the status of *MYC* and *PVT1* loci at 8q24. Dataset outputs were investigated using RStudio data analysis software. Further analyses were performed using OncoDB (17) and UALKAN (18, 19) online resources that utilize GTEX and TCGA datasets. Copy number variation for *MYC* and *PVT1* was assessed using cBioportal (20). Finally, the ROC Plotter was used to link gene expression with response to therapy (21).

Fluorescent in situ hybridization (FISH). FISH experiments on metaphase chromosomes and interphase nuclei were performed using a selection of probes mapping at different sites on the long arm of chromosome 8 (see Figure 1 for a list of probes and corresponding chromosomal locations). FISH experiments were carried

out as previously described (15, 22). Hybridization signals on metaphase chromosomes and interphase nuclei were analyzed using an Olympus AX70 fluorescence microscope, and images were captured using MacProbe v4.3 software (Applied Imaging, Newcastle, UK).

RP11-440N18 bacterial artificial chromosome (BAC) targeting MYC, RP11-125A17, and RP11-946L14 BAC probes targeting *PVT1* were used in FISH experiments. Probes were labelled directly with fluorochromes or indirectly with biotin or digoxigenin, using nick translation (Roche, Mannheim, Germany) and detected according to previously described standard methods (23). RP11-440N18 was directly labelled with FITC, RP11-125A17 labelled with CY3, whereas RP11-946L14 was labelled with biotin and detected with streptavidin-CY3.

Statistical analysis. The method used for differential analysis in the present study was one-way ANOVA, using disease state (Tumor or Normal) as variables for calculating differential expression: Gene expression ~disease state. The expression data were first log2 (TPM+1) transformed for differential analysis, and the log2FC was defined as median (Tumor) – median (Normal). Genes with higher |log2FC| values and lower q values than pre-set thresholds were considered differentially expressed genes.

Results

Expression and biomarker utility of MYC and PVT1 in ovarian cancer. Using the TCGA and GTEX datasets, it was demonstrated that, compared to the normal controls (n=180), *PVT1* and *MYC* expression levels remained unaltered in OC patients (n=418) (Figure 2A and Figure 3A). Putative copy number alterations across all cancers

showed a marked difference between the two genes, particularly in terms of gain and amplification for *MYC* (Figure 2B and Figure 3B). The expression of both genes was not dependent on the stage or *TP53* status (Figure 2C and D, Figure 3C and D). Finally, only *PVT1* demonstrated prognostic value for the treatment of patients with serous (n=1,624) and endometrioid (n=343) OC (Figure 2E and F, Figure 3E and F).

Correlation between MYC, PVT1, and chromosome 8 gene expression. To better understand any further "cross-talk", gene expression correlation was performed among all genes mapping on chromosome 8. By characterizing this chromosomal set, two genes, namely *PARP10* and *FAM83H,* were identified (Figure 4A). We further expanded our observations by creating a *PVT1-MYC* correlation heatmap in the TCGA cohort for the HUGO dataset, where a correlation with the *DEPTOR* gene was also noted (Figure 4B).

The *MYC* and *PVT1* copy number status assessment and its variation (CNV) in OC (25) was based on the TCGA ovarian gene levels dataset. The GISTIC2 method was applied on entire genome microarray datasets to produce segmented CNV data, which was then mapped to genes to make gene-level estimates. Genes were mapped onto the human genome coordinates using UCSC Xena HUGO probeMap. The information was obtained from 579 OC samples (Figure 5).

MYC and *PVT1* had the same CNV trend, which leads to rearrangements of the 8q24 chromosome band, harboring both genes. This result is in accordance with the literature; in fact, previous analyses of 15,241 tumors from the TCGA database showed that 18.02% (2,821 tumors) displayed 8q24 copy-number increase and that 2,746 out of 2,821 tumors (97.34%) showed co-gain of both *MYC* and *PVT1*. In

addition, less than 0.15% of tumors showed an increased copy number of *MYC* but not of *PVT1* (26).

Effects of rucaparib (PARP inhibitor) and MYC inhibitor in vitro. Three copies of chromosome 8 in the SKOV-3 cell line were observed using FISH with whole chromosome painting probes (data not shown). Furthermore, FISH using probes specific for the 8q24.21 region, encompassing the *MYC* and *PVT1* loci, showed that those genomic regions were retained in all three copies of chromosome 8 in the SKOV-3 cell line (Figure 1). Studies from our group have shown that 10 μM Rucaparib can induce apoptosis *in vitro*, not only in *BRCA2* mutant cells but also in those exhibiting "BRCAness", like those of the SKOV-3 cell line (27). This serous ovarian adenocarcinoma cancer cell line is one of the most frequently used in the scientific literature (28). Moreover, frequently mutated OC driver genes and copy number alterations have been described for this cell line (29).

Following the validation of SKOV3 as a preclinical model, we performed wound healing assays for up to 72 h to assess the combined impact of a PARP inhibitor (PARPi; Rucaparib) and a MYC inhibitor (MYCi; 10058-F4). A number of different concentrations of Rucaparib and MYCi were tested to determine whether these agents, alone or in combination, can exert a cytostatic or cytotoxic effect. It was evident that either inhibitor alone (data not shown) or in combination (*i.e.,* PARPi 12.5 μM and MYCi 2.5 μM) were capable of arresting cell growth (Figure 6). Higher concentrations resulted in complete cell death.

Following the *in vitro* studies, we assessed the impact of both Rucaparib (25 μM) and MYCi (10058F4; 10 μM) on the expression of linear (*PVT1*) and circular *PVT1* (circPVT1)*,* as well as the different *MYC* splicing variant transcripts. Both treatments

alone or in combination reduced the expression of *PVT1* and circPVT1 (Figure 7), as well as all *MYC* isoforms (Figure 8), compared to no treatment (basal) levels (p<0.05).

Discussion

In this study, we provide a comprehensive overview of the role of *MYC* and *PVT1* in OC, using both *in silico* and pre-clinical models. While neither of these genes appeared to have an altered expression in OC compared to controls or any TP53- or stage-dependent changes, their role is well-documented in cancer progression (30).

Although *PVT1* was not shown to have a diagnostic potential, it might have a clinical utility as a prognostic biomarker, given that patients with OC who do not respond to treatment have higher *PVT1* expression. Several studies have indicated an involvement of *PVT1* in radio- and chemo-resistance (31). For example, when *PVT1* was over-expressed *in vitro* (in SKOV3 and A2780 cell lines), it promoted cisplatin resistance in a pathway that involved apoptotic components like caspase-3 (32). A similar study corroborated these findings, although the authors have demonstrated the involvement of the miR-370/FOXM1 pathway (33). These data collectively argue for targeting *PVT1* to reverse chemoresistance in OC.

It is well known that *PVT1* expression correlates with that of MYC (31). Here, we provide further insight into chromosome 8 gene correlations. Three genes, namely *PARP10, FAM83H,* and *DEPTOR,* demonstrated a good correlation. *PARP10* is over-expressed in numerous cancers, including OC, and can be a driver of tumorigenesis and promote cellular proliferation (34). Moreover, Saha *et al*. have identified PARP10 as a novel marker of platinum response in OC patients (35). Similarly, *FAM38H*

appears to be significantly over-expressed in OC, correlated with the FIGO stage, and involved in cancer progression *via* a cell-cycle signaling pathway (36). Using esophageal cancer cell lines, Feng *et al.* have shown that FAM38H-AS1 is involved in epithelial-to-mesenchymal transition (EMT), a fundamental process for cancer progression (37). To date, there is no data on the involvement of this lncRNA in the EMT process in OC. Finally, a correlation with *DEPTOR* was also noted. This result is increasingly important, given the involvement of mTOR signaling in cancer. We studied extensively the role of mTORC1 and mTORC2 components in OC and how paralogues can be used therapeutically (38-40). Although initial studies suggested that *DEPTOR* can act as a suppressor of mTOR, the relationship with mTORC1 and mTORC2 appears to be far more complex (41). Moreover, in colorectal cancer, *DEPTOR* is a target for MYC since it can bind directly to the *DEPTOR* promoter region and subsequently regulate its transcription (24). Despite the lack of studies showing any mechanistic involvement of *PVT1* in the *DEPTOR* expression, a survey on patients with Li-Fraumeni-like syndrome (LFLS) showed co-amplification of both genes at 8q24.2, suggesting their involvement in LFLS-associated tumors (25).

In the second part of the study, we assessed the effects of Rucaparib (a PARP inhibitor) in the presence or absence of 10058-F4 (a MYC inhibitor) *in vitro*. Poly(ADP-ribose) polymerase (PARP) inhibitors are now used therapeutically in patients with OC harboring homologous recombination repair deficiencies (HRD). Rucaparib is an oral PARP inhibitor that has shown promising results. In a recent randomized, phase III clinical trial, Rucaparib monotherapy appeared effective as first-line maintenance therapy in HRD-positive and negative PC patients (42). However, to date, no clinical trials have used 10058-F4 for intervention in any cancer (source: clinicaltrials.gov).

When we performed a wound healing assay, both compounds appeared to exert a strong, not additive, cytostatic/ cytotoxic effect *in vitro*. Data from Rucaparib treatment corroborates our previous study on a wider repertoire of OC cell lines, where we have demonstrated that Rucaparib significantly decreased cell proliferation (27). Similar results have been previously recorded with the use of the MYC inhibitor. For example, treatment of 2008C13 OC cells with 10058-F4 induced cell cycle arrest at the G1 phase and stimulated the expression of cell-cycle related genes (*e.g.*, p15, p21) (43).

Study limitations. We only performed the experiments in one cell line. Future studies should use a broader range of concentrations and more cell lines representative of high-grade and low-grade serous cancers, as well as cells that have mutations in either *BRCA1* or *BRCA2*, where Rucaparib should exert a more significant effect *via* synthetic lethality. *In silico* tools can also be restrictive in the case of *MYC*, due to the expression of multiple isoforms. Future investigations should also concentrate on further functional studies in combination with omics approaches to define the exact pathway(s) involved in these responses. Furthermore, our data further underpin a role for *PVT1* in the response to treatment. It is necessary, therefore, to develop *PVT1* inhibitors that can be used in combination with other chemotherapeutic agents (*e.g.,* cisplatin, taxol) that can reduce the onset of chemoresistance. More work is needed to gain a much deeper insight into how druggable these genes are prior to embarking on clinical trials.

Conclusion

We assessed the effect of both PARP- and MYC-inhibitors on *PVT1*, circPVT1, and *MYC* transcript isoforms using RT-qPCR. All treatments, in combination or as monotherapies, significantly decreased all tested transcripts of the genes mentioned

above. Again, similarly to the wound healing assay, the effect was not synergistic when both inhibitors were used. To the best of our knowledge, this is the first time that the impact of these inhibitors is assessed in terms of *PVT1* or *MYC* expression and suggests another way that they can exert their anti-tumor effects.

Conflicts of Interest

The Authors declare no competing interests in relation to this study.

Authors' Contributions

Conceptualization, ST, EK, CTS; Methodology, AM, SS, CS, ST, EK; Validation, ST.; Formal Analysis, AM, CS, SS, EK; Draft preparation, ST, EK, CTS; writing—review and editing, AM, SS, CS, MH, ST, EK, CTS; visualization, AM, SS, CS; supervision, MH, ST, EK, and CTS. EK and CTS are joint senior and corresponding co-Authors; AM and SS are joined first co-authors.

Funding

This study was partially funded through the Cancer Treatment & Research Trust (CTRT), and the Global Thesis Program 2017-2018 (University of Bari Aldo Moro).

References

1 Guan Y, Kuo WL, Stilwell JL, Takano H, Lapuk AV, Fridlyand J, Mao JH, Yu M, Miller MA, Santos JL, Kalloger SE, Carlson JW, Ginzinger DG, Celniker SE, Mills GB, Huntsman DG, Gray JW: Amplification of PVT1 contributes to the pathophysiology of ovarian and breast cancer. Clin Cancer Res 13: 5745–5755, 2007. DOI: 10.1158/1078-0432.CCR-06-2882

2 Garte SJ: The c-myc oncogene in tumor progression. Crit Rev Oncog 4: 435–449, 1993.

3 Dimova I, Raitcheva S, Dimitrov R, Doganov N, Toncheva D: Correlations between c-myc gene copy-number and clinicopathological parameters of ovarian tumours. Eur J Cancer 42: 674–679, 2006. DOI: 10.1016/j.ejca.2005.11.022

4 Barsotti AM, Beckerman R, Laptenko O, Huppi K, Caplen NJ, Prives C: p53-Dependent induction of PVT1 and miR-1204. J Biol Chem 287: 2509–2519, 2012. DOI: 10.1074/jbc.M111.322875

5 Shigeyasu K, Toden S, Ozawa T, Matsuyama T, Nagasaka T, Ishikawa T, Sahoo D, Ghosh P, Uetake H, Fujiwara T, & Goel A: The PVT1 lncRNA is a novel epigenetic enhancer of MYC, and a promising risk-stratification biomarker in colorectal cancer. Mol Cancer 19: 155, 2020. DOI: 10.1186/s12943-020-01277-4

6 Shtivelman E, Bishop JM: The PVT gene frequently amplifies with MYC in tumor cells. Mol Cell Biol 9: 1148–1154, 1989. DOI: 10.1128/mcb.9.3.1148-1154.1989

7 E Shtivelman E, Bishop JM: Effects of translocations on transcription from PVT. Mol Cell Biol 10: 1835–1839, 1990. DOI: 10.1128/mcb.10.4.1835-1839.1990

8 Shtivelman E, Henglein B, Groitl P, Lipp M, Bishop JM: Identification of a human transcription unit affected by the variant chromosomal translocations 2;8 and 8;22 of Burkitt lymphoma. Proc Natl Acad Sci USA 86: 3257–3260, 1989. DOI: 10.1073/pnas.86.9.3257

9 Abbate AL, Tolomeo D, Cifola I, Severgnini M, Turchiano A, Augello B, Squeo G, D Addabbo P, Traversa D, Daniele G, Lonoce A, Pafundi M, Carella M, Palumbo O, Dolnik A, Muehlematter D, Schoumans J, Van Roy N, De Bellis G, Martinelli G, Merla G, Bullinger L, Haferlach C, Storlazzi CT: MYC-containing amplicons in acute

myeloid leukemia: genomic structures, evolution, and transcriptional consequences. Leukemia 32: 2152–2166, 2018. DOI: 10.1038/s41375-018-0033-0

10 Tolomeo D, Traversa D, Venuto S, Ebbesen KK, García Rodríguez JL, Tamma G, Ranieri M, Simonetti G, Ghetti M, Paganelli M, Visci G, Liso A, Kok K, Muscarella LA, Fabrizio FP, Frassanito MA, Lamanuzzi A, Saltarella I, Solimando AG, Fatica A, Ianniello Z, Marsano RM, Palazzo A, Azzariti A, Longo V, Tommasi S, Galetta D, Catino A, Zito A, Mazza T, Napoli A, Martinelli G, Kjems J, Kristensen LS, Vacca A, Storlazzi CT: circPVT1 and PVT1/AKT3 show a role in cell proliferation, apoptosis, and tumor subtype-definition in small cell lung cancer. Genes Chromosomes Cancer 62: 377–391, 2023. DOI: 10.1002/gcc.23121

11 L Abbate A, Tolomeo D, Cifola I, Severgnini M, Turchiano A, Augello B, Squeo G, D Addabbo P, Traversa D, Daniele G, Lonoce A, Pafundi M, Carella M, Palumbo O, Dolnik A, Muehlematter D, Schoumans J, Van Roy N, De Bellis G, Martinelli G, Merla G, Bullinger L, Haferlach C, Storlazzi CT: MYC-containing amplicons in acute myeloid leukemia: genomic structures, evolution, and transcriptional consequences. Leukemia 32: 2152–2166, 2018. DOI: 10.1038/s41375-018-0033-0

12 Palcau AC, Canu V, Donzelli S, Strano S, Pulito C, Blandino G: CircPVT1: a pivotal circular node intersecting long non-coding-PVT1 and c-MYC oncogenic signals. Mol Cancer 21: 33, 2022. DOI: 10.1186/s12943-022-01514-y

13 Chen Y, Du H, Bao L, Liu W: LncRNA PVT1 promotes ovarian cancer progression by silencing miR-214. Cancer Biol Med 15: 238–250, 2018. DOI: 10.20892/j.issn.2095-3941.2017.0174

14 Howlader N, Noone AM, Krapcho M, Miller D, Bishop K, Kosary CL, Yu M, Ruhl J, Tatalovich Z, Mariotto A, Lewis DR, Chen HS, Feuer EJ, Cronin KA (eds): Lifetime risk (Percent) of being diagnosed with cancer by site and race/ethnicity; Males, 18

SEER Areas, 2012-2014 SEER Cancer Statistics Review, 1975-2014. National Cancer Institute, 2017. https://seer.cancer.gov/csr/1975_2014/

15 Garimberti E, Tosi S: Fluorescence in situ hybridization (FISH), basic principles and methodology. Methods Mol Biol 659: 3–20, 2010. DOI: 10.1007/978-1-60761-789-1_1

16 Schmittgen TD, Livak KJ: Analyzing real-time PCR data by the comparative C(T) method. Nat Protoc 3: 1101–1108, 2008. DOI: 10.1038/nprot.2008.73

17 Tang G, Cho M, Wang X. OncoDB: an interactive online database for analysis of gene expression and viral infection in cancer. Nucleic Acids Res 50: D1334–D1339, 2022. DOI: 10.1093/nar/gkab970

18 Chandrashekar DS, Karthikeyan SK, Korla PK, Patel H, Shovon AR, Athar M, Netto GJ, Qin ZS, Kumar S, Manne U, Creighton CJ, Varambally S: UALCAN: An update to the integrated cancer data analysis platform. Neoplasia 25: 18–27, 2022. DOI: 10.1016/j.neo.2022.01.001

19 Chandrashekar DS, Bashel B, Balasubramanya SAH, Creighton CJ, Ponce-Rodriguez I, Chakravarthi BVSK, Varambally S: UALCAN: A portal for facilitating tumor subgroup gene expression and survival analyses. Neoplasia 19: 649–658, 2017. DOI: 10.1016/j.neo.2017.05.002

20 Cerami E, Gao J, Dogrusoz U, Gross BE, Sumer SO, Aksoy BA, Jacobsen A, Byrne CJ, Heuer ML, Larsson E, Antipin Y, Reva B, Goldberg AP, Sander C, Schultz N: The cBio cancer genomics portal: an open platform for exploring multidimensional cancer genomics data. Cancer Discov 2: 401–404, 2012. DOI: 10.1158/2159-8290.CD-12-0095

21 Fekete JT, Győrffy B: ROCplot.org: Validating predictive biomarkers of chemotherapy/hormonal therapy/anti-HER2 therapy using transcriptomic data of

3,104 breast cancer patients. Int J Cancer 145: 3140–3151, 2019. DOI: 10.1002/ijc.32369

22 Federico C, Cantarella CD, Di Mare P, Tosi S, Saccone S: The radial arrangement of the human chromosome 7 in the lymphocyte cell nucleus is associated with chromosomal band gene density. Chromosoma 117: 399-410, 2008. DOI: 10.1007/s00412-008

23 Federico C, Pappalardo AM, Ferrito V, Tosi S, Saccone S: Genomic properties of chromosomal bands are linked to evolutionary rearrangements and new centromere formation in primates. Chromosome Res 25: 261–276, 2017. DOI: 10.1007/s10577-017-9560-1

24 Wang Q, Zhou Y, Rychahou P, Harris JW, Zaytseva YY, Liu J, Wang C, Weiss HL, Liu C, Lee EY, Evers BM: Deptor is a novel target of Wnt/β-Catenin/c-Myc and contributes to colorectal cancer cell growth. Cancer Res 78: 3163–3175, 2018. DOI: 10.1158/0008-5472.CAN-17-3107

25 Sugawara W, Arai Y, Kasai F, Fujiwara Y, Haruta M, Hosaka R, Nishida K, Kurosumi M, Kobayashi Y, Akagi K, Kaneko Y: Association of germline or somatic TP53 missense mutation with oncogene amplification in tumors developed in patients with Li-Fraumeni or Li-Fraumeni-like syndrome. Genes Chrom Cancer 50: 535–545, 2011. DOI: 10.1002/gcc.20878

26 Tseng YY, Moriarity BS, Gong W, Akiyama R, Tiwari A, Kawakami H, Ronning P, Reuland B, Guenther K, Beadnell TC, Essig J, Otto GM, O'Sullivan MG, Largaespada DA, Schwertfeger KL, Marahrens Y, Kawakami Y, Bagchi A: PVT1 dependence in cancer with MYC copy-number increase. Nature 512: 82–86, 2014. DOI: 10.1038/nature13311

27 Saravi S, Alizzi Z, Tosi S, Hall M, Karteris E: Preclinical studies on the effect of rucaparib in ovarian cancer: Impact of Brca2 status. Cells 10: 2434, 2021. DOI: 10.3390/cells10092434

28 Kerslake R, Belay B, Panfilov S, Hall M, Kyrou I, Randeva HS, Hyttinen J, Karteris E, Sisu C: Transcriptional landscape of 3D vs. 2D ovarian cancer cell models. Cancers (Basel) 15: 3350, 2023. DOI: 10.3390/cancers15133350

29 Li J, Chen Z, Xiao W, Liang H, Liu Y, Hao W, Zhang Y, Wei F: Chromosome instability region analysis and identification of the driver genes of the epithelial ovarian cancer cell lines A2780 and SKOV3. J Cell Mol Med 27: 3259–3270, 2023. DOI: 10.1111/jcmm.17893

30 Yao W, Li S, Liu R, Jiang M, Gao L, Lu Y, Liang X, Zhang H: Long non-coding RNA PVT1: A promising chemotherapy and radiotherapy sensitizer. Front Oncol 12: 959208, 2022. DOI: 10.3389/fonc.2022.959208

31 Tabury K, Monavarian M, Listik E, Shelton AK, Choi AS, Quintens R, Arend RC, Hempel N, Miller CR, Györrfy B, Mythreye K: PVT1 is a stress-responsive lncRNA that drives ovarian cancer metastasis and chemoresistance. Life Sci Alliance 5: e202201370, 2022. DOI: 10.26508/lsa.202201370

32 Liu E, Liu Z, Zhou Y, Mi R, Wang D: Overexpression of long non-coding RNA PVT1 in ovarian cancer cells promotes cisplatin resistance by regulating apoptotic pathways. Int J Clin Exp Med 8: 20565–20572, 2015.

33 Yi K, Hou M, Yuan J, Yang L, Zeng X, Xi M, Chen J: LncRNA PVT1 epigenetically stabilizes and post-transcriptionally regulates FOXM1 by acting as a microRNA sponge and thus promotes malignant behaviors of ovarian cancer cells. Am J Transl Res 12: 2860–2874, 2020.

34 Schleicher EM, Galvan AM, Imamura-Kawasawa Y, Moldovan GL, Nicolae CM: PARP10 promotes cellular proliferation and tumorigenesis by alleviating replication stress. Nucleic Acids Res 46: 8908–8916, 2018. DOI: 10.1093/nar/gky658

35 Sharma Saha S, Gentles L, Bradbury A, Brecht D, Robinson R, O'Donnell R, Curtin NJ, Drew Y: Genomic, transcriptomic, and functional alterations in DNA damage response pathways as putative biomarkers of chemotherapy response in ovarian cancer. Cancers (Basel) 13: 1420, 2021. DOI: 10.3390/cancers13061420

36 Lin S, Du J, Hao J, Luo X, Wu H, Zhang H, Zhao X, Xu L, Wang B: Identification of prognostic biomarkers among FAM83 family genes in human ovarian cancer through bioinformatic analysis and experimental verification. Cancer Manag Res 13: 8611–8627, 2021. DOI: 10.2147/CMAR.S328851

37 Feng B, Wang G, Liang X, Wu Z, Wang X, Dong Z, Guo Y, Shen S, Liang J, Guo W: LncRNA FAM83H-AS1 promotes oesophageal squamous cell carcinoma progression via miR-10a-5p/Girdin axis. J Cell Mol Med 24: 8962–8976, 2020. DOI: 10.1111/jcmm.15530

38 Rogers-Broadway KR, Chudasama D, Pados G, Tsolakidis D, Goumenou A, Hall M, Karteris E: Differential effects of rapalogues, dual kinase inhibitors on human ovarian carcinoma cells in vitro. Int J Oncol 49: 133–43, 2016. DOI: 10.3892/ijo.2016.3531

39 Rogers-Broadway KR, Kumar J, Sisu C, Wander G, Mazey E, Jeyaneethi J, Pados G, Tsolakidis D, Klonos E, Grunt T, Hall M, Chatterjee J, Karteris E: Differential expression of mTOR components in endometriosis and ovarian cancer: Effects of rapalogues and dual kinase inhibitors on mTORC1 and mTORC2 stoichiometry. Int J Mol Med 43: 47–56, 2019. DOI: 10.3892/ijmm.2018.3967

40 Foster H, Coley HM, Goumenou A, Pados G, Harvey A, Karteris E: Differential expression of mTOR signalling components in drug resistance in ovarian cancer. Anticancer Res 30: 3529–3534, 2010.

41 Caron A, Briscoe DM, Richard D, Laplante M: DEPTOR at the nexus of cancer, metabolism, and immunity. Physiol Rev 98: 1765–1803, 2018. DOI: 10.1152/physrev.00064.2017

42 Monk BJ, Parkinson C, Lim MC, O'Malley DM, Oaknin A, Wilson MK, Coleman RL, Lorusso D, Bessette P, Ghamande S, Christopoulou A, Provencher D, Prendergast E, Demirkiran F, Mikheeva O, Yeku O, Chudecka-Glaz A, Schenker M, Littell RD, Safra T, Chou HH, Morgan MA, Drochýtek V, Barlin JN, Van Gorp T, Ueland F, Lindahl G, Anderson C, Collins DC, Moore K, Marme F, Westin SN, McNeish IA, Shih D, Lin KK, Goble S, Hume S, Fujiwara K, Kristeleit RS: A randomized, phase III trial to evaluate rucaparib monotherapy as maintenance treatment in patients with newly diagnosed ovarian cancer (ATHENA-MONO/GOG-3020/ENGOT-ov45). J Clin Oncol 40: 3952–3964, 2022. DOI: 10.1200/JCO.22.01003

43 Ghaffarnia R, Nasrollahzadeh A, Bashash D, Nasrollahzadeh N, Mousavi SA, Ghaffari SH: Inhibition of c-Myc using 10058-F4 induces anti-tumor effects in ovarian cancer cells via regulation of FOXO target genes. Eur J Pharmacol 908: 174345, 2021. DOI: 10.1016/j.ejphar.2021.174345

Table I. Primers used in RT-qPCR experiments.

Gene name	**Orientation**	**Sequence**
YWHAZ	Forward	5′-AGACGGAAGGTGCTGAGAAA-3′
	Reverse	5′-GAAGCATTGGGGATCAAGAA-3′
Linear PVT1	Forward	5′-GCCTGATCTTTTGGCCAGAAGGAG-3′
	Reverse	5′-CTCAAGCCCAGCTGAGCGCCGGATG-3′
Circular PVT1	Forward	5′-GGTTCCACCAGCGTTATTC-3′
	Reverse	5′-CAACTTCCTTTGGGTCTCC-3′
MYC-ucbbe1	Forward	5′-GCTGCTTAGACGCTGGATTT-3′
	Reverse	5′-TCCTGTTGGTGAAGCTAACG-3′
	Forward	5′-TGCTCCATGAGGAGACACC-3′

MYC-ucbbe2	Reverse	5′-GCCTCTTTTCCACAGAAACAA-3′
MYC-ucysh1	Forward	5′-GAGCAGCAGAGAAAGGGAGA-3′
	Reverse	5′-GCTCGGGTGTTGTAAGTTCC-3′

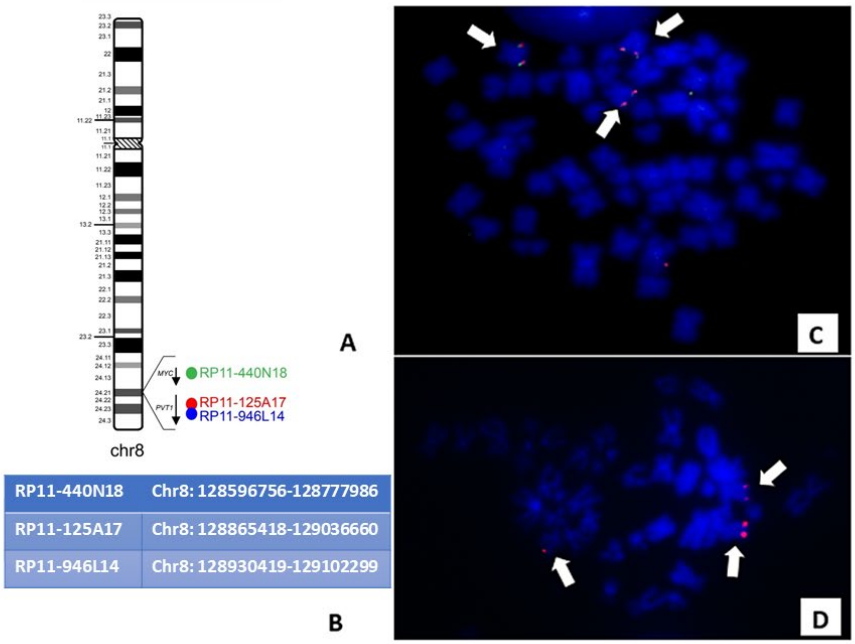

Figure 1. Fluorescence in situ hybridization on SKOV-3 metaphase chromosomes. Localization of genomic regions covered by FISH probes used in this study as shown on the ideogram of chromosome 8 (A) and with reference to the genomic positions according to the GRCh37/hg19 release of the UCSC Human Genome Browser (B). Dual color FISH using probes RP11-440N18-FITC (green) and RP11-125A17-CY3 (red) shows the presence of signals for both probes in the three copies of chromosome 8 (C). Single color FISH using probe RP11-946L14 (detected using streptavidin-Cy3, visible in red) also shows the presence of signals in each one of the three copies of chromosome 8 (D).

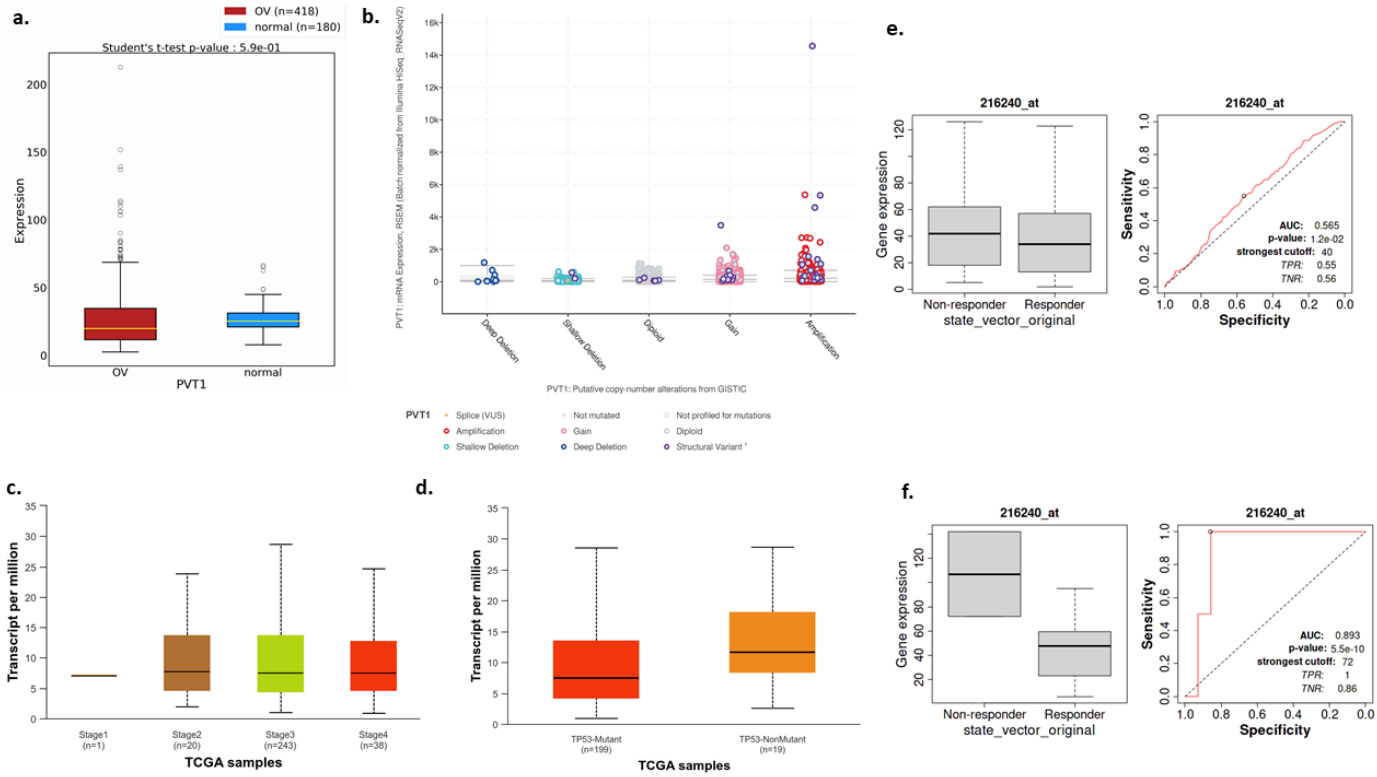

Figure 2. *PVT1* expression in ovarian cancer (OC). **A)** *PVT1* expression between normal (n=180) and OC patients (OV, n=418)); **B)** putative copy-number of *PVT1* alterations from GISTIC (across all cancers); **C)** *PVT1* expression in OC across different stages (I-IV); **D)** *PVT1* expression in OC according to p53 status; **E)** non-responders (n=492) to treatment serous OC patients have higher expression of *PVT1* compared to responders (n=1138); and **F)** non-responders (n=142) to treatment of endometrioid OC patients have higher expression of *PVT1* compared to responders (n=201).

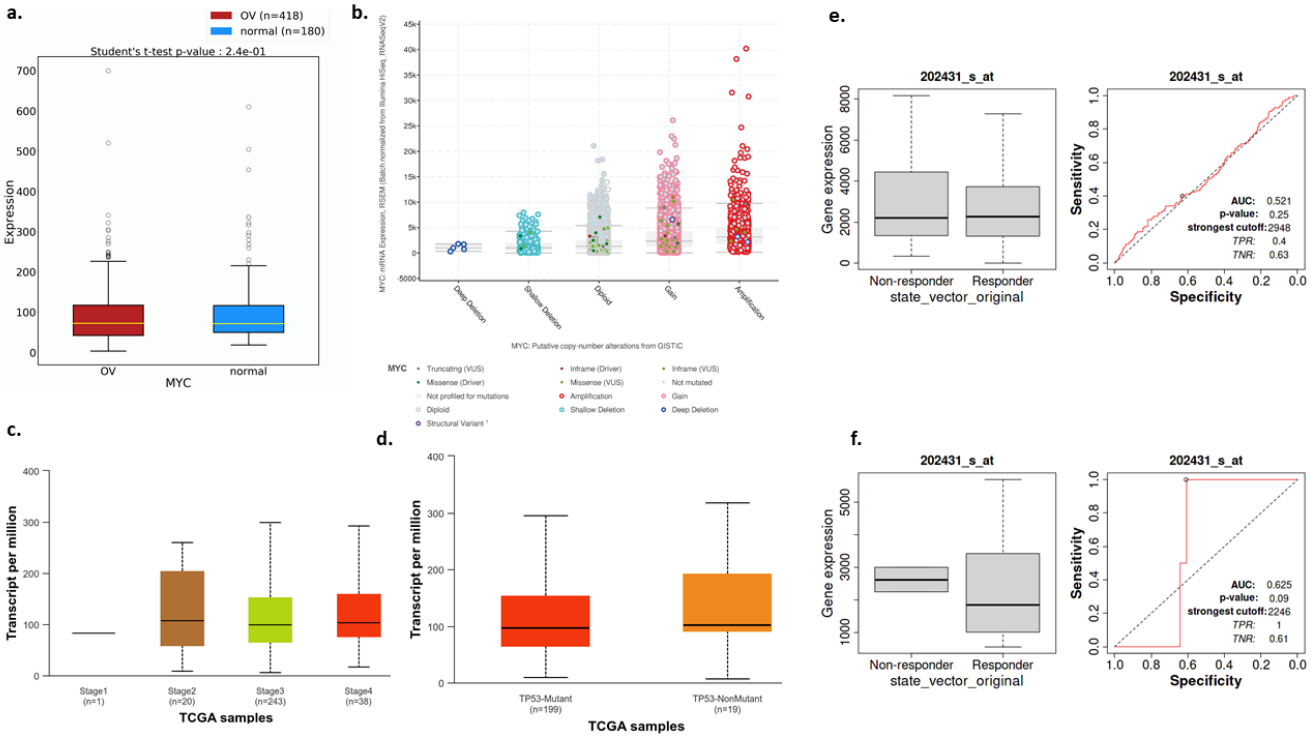

Figure 3. *MYC1* expression in ovarian cancer (OC). **A)** *MYC* expression between normal and OC (OV) patients; **B)** putative copy-number of *MYC* alterations from GISTIC (across all cancers); **C)** *MYC* expression in OC across different stages (I-IV); **D)** *MYC* expression in OC according to p53 status; **E)** non-responders to treatment serous OC patients have higher expression of *MYC*; and **F)** non-responders to treatment endometrioid OC patients have higher expression of *MYC*.

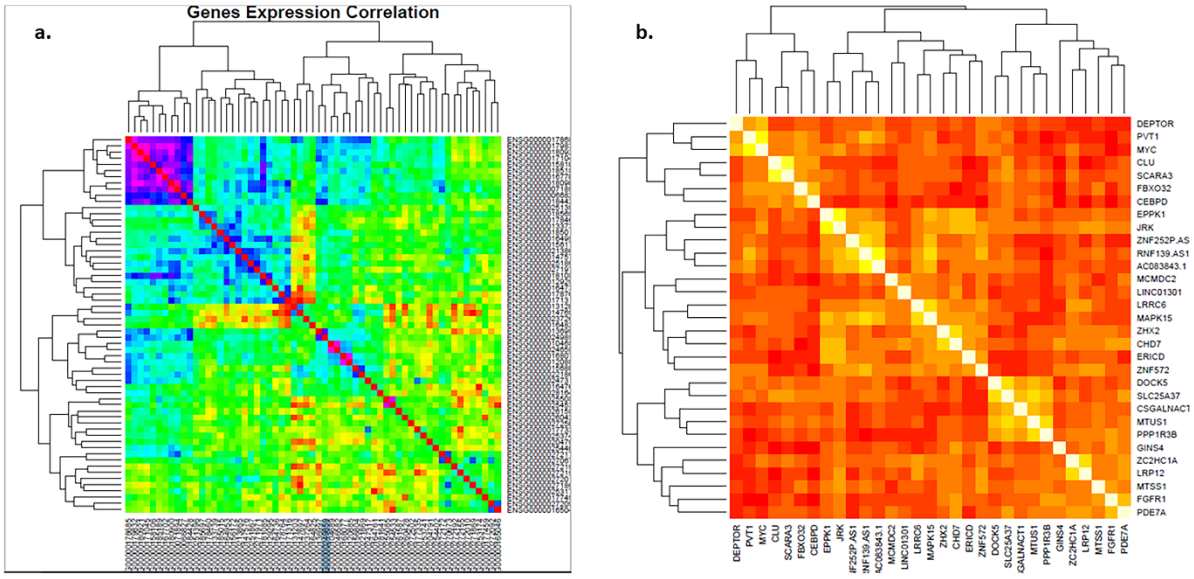

Figure 4. Heatmap for Chromosome 8 gene expression correlation in TCGA (**A**); and HUGO (**B**) (25).

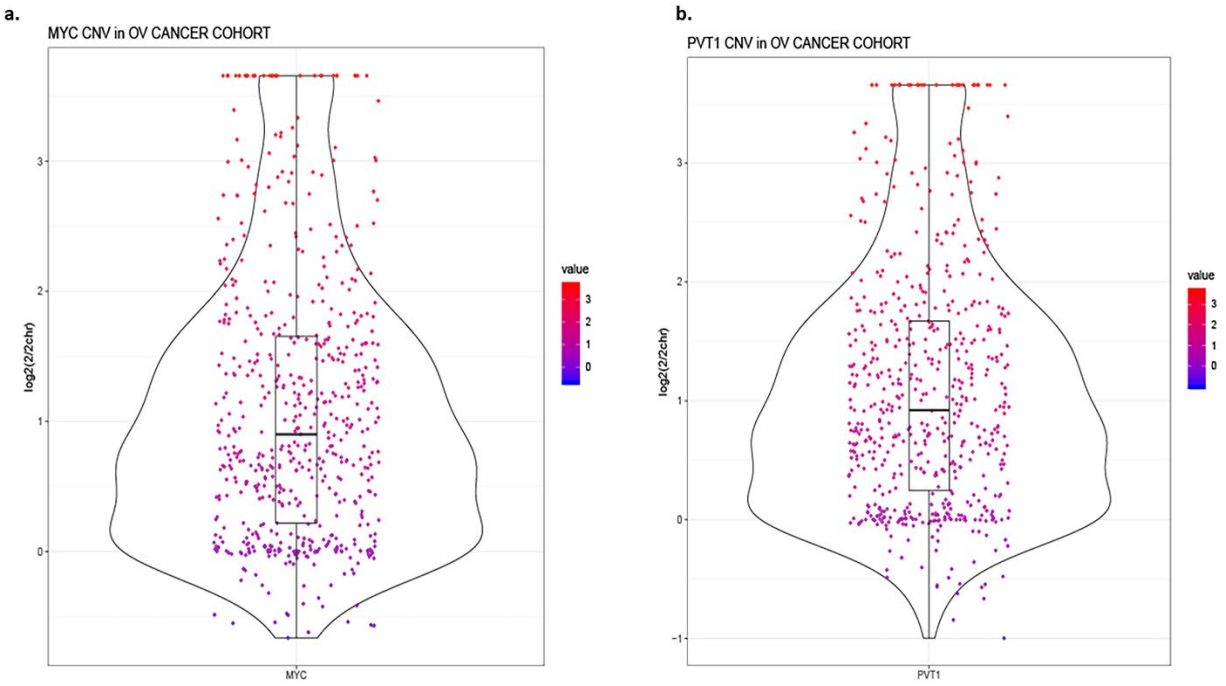

Figure 5. Copy number variation of MYC and PVT1. Analyses of 15,241 tumors from the TCGA database showed that 18.02% (2,821 tumors) displayed 8q24 copy-number increase and that 2,746 out of 2,821 tumors (97.34%) showed co-gain of both MYC (**A**) and PVT1 (**B**). CNV: Copy number variation; OV: ovarian cancer.

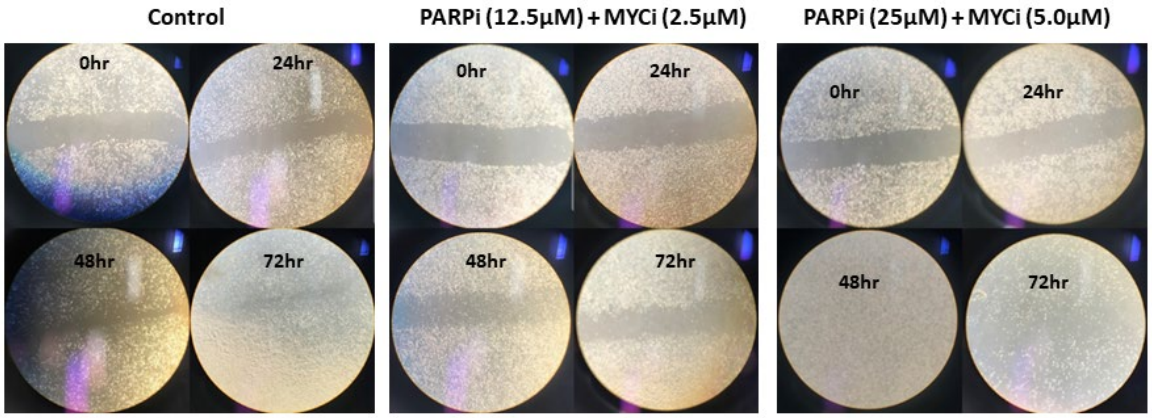

Figure 6. Schematic representation showings the healing of the artificial wound on all cell line surfaces (40× magnification). The figure shows the cells before (0-h) and after treatment at 24, 48, and 72 h. The images show the extent of the scratch closure developed under control conditions compared to those following treatment with PARPi (12.5 µM) and MYCi (2.5 µM), and treated cells with PARPi (25 µM) and MYCi (5.0 µM).

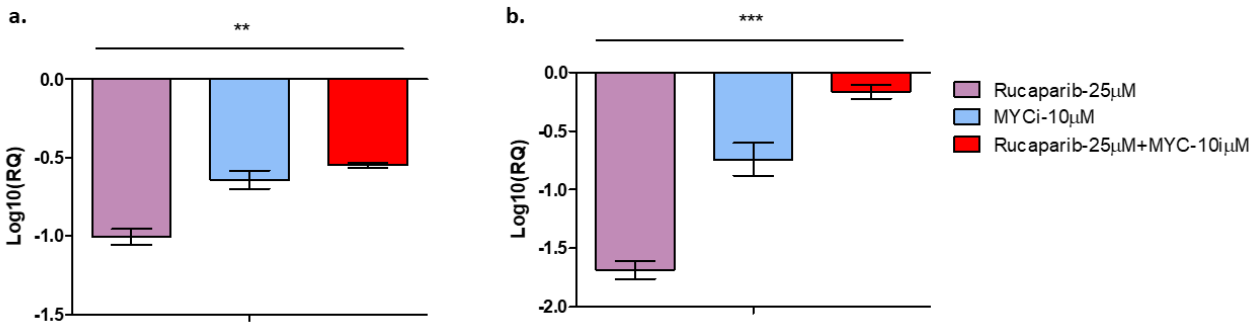

Figure 7. Effect of the Rucaparib (25 μM) and MYCi (10058F4; 10 μM) on the gene expression of *PVT1* (**A**) and circPVT1 (**B**). In both cases, both treatments alone or in combination reduced significantly (p<0.005) the expression of *PVT1* transcripts. For the *PVT1*, Rucaparib alone exerted a more significant decrease compared to MYCi or in combination with MYCi (p=0.0024; Panel **A**). Similarly, for the circPVT1, Rucaparib alone exerted a significant decrease compared to MYCi or in combination with MYCi (p=0.0009; Panel **B**). Error bars: SEM.

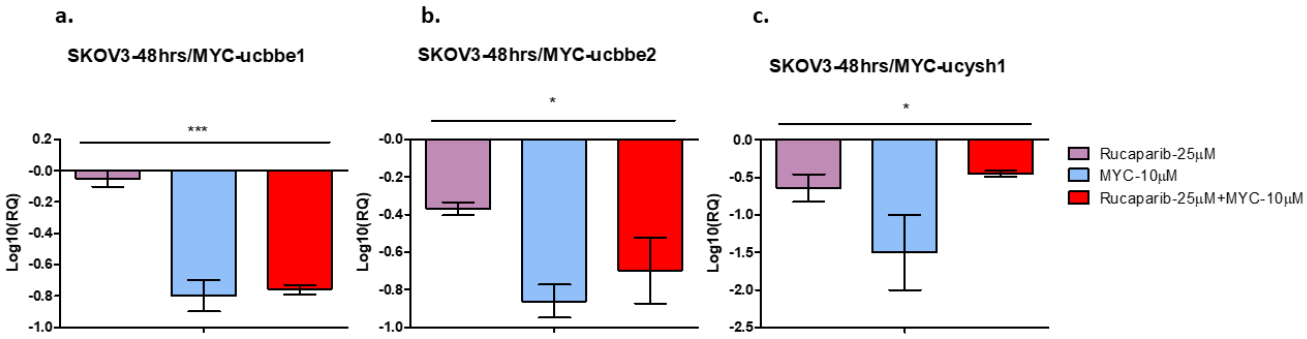

Figure 8. Effect of the Rucaparib (25 μM) and MYCi (10058F4; 10 μM) on the gene expression of all *MYC* splicing variants (panels **A, B, C**). In all cases, both treatments alone or in combination significantly reduced the expression of the *MYC* isoforms (**p*<0.05; ****p*<0.001). Error bars: SEM.